EJP
European Journal of Pain

ORIGINAL ARTICLE

Pulsed radiofrequency inhibited activation of spinal mitogen-activated protein kinases and ameliorated early neuropathic pain in rats

M.-L. Lin[1,2,#], W.-T. Lin[3,#], R.-Y. Huang[4], T.-C. Chen[1], S.-H. Huang[5], C.-H. Chang[1], S.-Y. Tsai[6], H.-W. Chiu[7], G.-C. Yeh[8], C.-W. Lin[1,3]*, Y.-R. Wen[6,9,10,11]*

1 Institute of Biomedical Engineering, National Taiwan University, Taipei, Taiwan
2 Pain Center, Zhongxing Branch of Taipei City Hospital, Taipei, Taiwan
3 Institute of Biomedical Electronics and Bioinformatics, National Taiwan University, Taipei, Taiwan
4 Graduate Institute of Clinical Medical Science, China Medical University, Taichung, Taiwan
5 Department of Anesthesiology, Shin-Kong Wu-Ho-Su Memorial Hospital, Taipei, Taiwan
6 Department of Anesthesiology, School of Medicine, China Medical University, Taichung, Taiwan
7 Graduate Institute of Computer and Communication Engineering, National Taipei University of Technology, Taiwan
8 Department of Pediatrics, School of Medicine, Taipei Medical University, Taiwan
9 Department of Anesthesiology, China Medical University Hospital, Taichung, Taiwan
10 Center for Pain Management and Research, China Medical University Hospital, Taichung, Taiwan
11 Graduate Institute of Acupuncture Science, College of Chinese Medicine, China Medical University, Taichung, Taiwan

Correspondence
Yeong-Ray Wen
E-mail: yray.wen@mail.cmu.edu.tw; yr.wen@yahoo.com.tw

Funding sources
This study was sponsored by research grants from the National Science Council in Taiwan (NSC 99–2628-B-341-001-MY2) and the Center of Excellence for Clinical Trial and Research in Neuroscience, Taipei Medical University (DOH99-TD-B-111-003) to Y.-R. Wen, and grants from National Taiwan University (98E3107) and the National Science Council in Taiwan (NSC 99–2321-B-002–034) to C.-W. Lin.

Conflicts of interest
None declared.

#M.-L. Lin and W.-T. Lin have contributed equally in this study.

*C.-W. Lin and Y.-R. Wen made equal contributions as the corresponding authors in this study.

Part of the data had been presented in poster form in EFIC 2011.

Accepted for publication
10 September 2013

doi:10.1002/j.1532-2149.2013.00419.x

Abstract

Background: Pulsed radiofrequency (PRF) has been widely used to treat chronic pain, but the effectiveness and mechanisms in preventing early neuropathic pain have not been well explored. Even fewer knowledge is available in its impact on glia-mediated nociceptive sensitization. This study aims to elucidate the modulation of PRF on nerve injury-induced pain development and activation of spinal mitogen-activated protein kinases (MAPKs).

Methods: In a rat spinal nerve ligation (SNL) model, a low-volt PRF treatment was applied to the L5 dorsal root ganglion after nerve injury. Nociceptive behaviours were measured by von Frey and heat withdrawal tests at multiple time points. MAPK activations, including p-ERK and p-p38, as well as TNF-α level in the spinal dorsal horn were assessed and the cell types that expressed MAPK activation were identified by double immunofluorescence staining.

Results: We found that SNL promptly induced neuropathic pain in the affected hind limb for over 1 week as well as increased p-ERK and p-p38 in the spinal dorsal horn. PRF significantly attenuated SNL-induced mechanical allodynia and thermal hyperalgesia for 5–7 days. PRF also inhibited ERK and p38 activations, which were found majorly located within neurons and microglia, respectively. Besides, PRF significantly suppressed expression of TNF-α in the spinal dorsal horn throughout the course.

Conclusions: Low-volt PRF significantly ameliorated SNL-induced acute pain. Inferentially, PRF may inhibit spinal sensitization by down-regulating spinal MAPK activations and activation-mediated cytokine release. We demonstrated that early PRF treatment in acute nerve injury helps to ameliorate neuropathic pain development.

What's already known about this topic?

- Clinically, pulsed radiofrequency (PRF) attenuates chronic neuropathic pain. Basic studies proved that PRF causes minimal and reversible destruction on nervous system, but underlying analgesic mechanisms were unsolved. Moreover, effect of PRF on acute neuropathic pain has not been clearly elucidated.

What does this study add?

- A low-volt bipolar PRF produced prolonged analgesia on acute neuropathic pain in rats.
- PRF down-regulated injury-induced mitogen-activated protein kinase activations within spinal neurons and glia, and inhibited glia-mediated nociceptive sensitization.

1. Introduction

All chronic forms of pain are acute at their inception – it is the passage of time that transforms the states. Neuropathic pain is usually regarded as a constellation of chronic pain symptoms (Treede et al., 2008), but in fact these peculiar pains occur early after direct nervous damage. Clinical experiences and basic studies have stressed the importance to halt an evolution from acute to chronic; nevertheless, how to manage acute neuropathic pain remains a challenge and has not been profoundly explored (Gray, 2008).

Pulsed radiofrequency (PRF) has been widely used as a non-pharmacological alternative in treating difficult neuropathic pain (van Boxem et al., 2008). Because of the minimally destructive property, PRF could avoid motor deficits that were commonly seen after conventional radiofrequency (Sluijter et al., 1998; Sluijter, 2000). Although accumulating studies indicated that PRF treatment at the dorsal root ganglion (DRG) can effectively ameliorate neck and low back radicular pain (Van Boxem et al., 2010; Van Zundert et al., 2010; Chua et al., 2011), underlying molecular mechanisms for analgesic effect are largely unclear.

PRF was traditionally considered to be non-destructive (Sluijter et al., 1998). Nevertheless, current evidence indicates that PRF applied onto DRG caused focal oedematous changes in mitochondria, pore formation in cellular membranes and myelin separation in myelinated axons (Erdine et al., 2005, 2009; Tun et al., 2006, 2009; Protasoni et al., 2009). These changes are often reversible and relatively minor (Podhajsky et al., 2005). Fos expression was also induced in the superficial dorsal horn (i.e. laminae I and II) immediately (3 h) and up to 7 days after PRF stimulation, suggesting a long-lasting spinal neuronal activity (Higuchi et al., 2002; Van Zundert et al., 2005). Besides, PRF was shown to produce long-term depression through enhancement of noradrenergic and serotonergic descending inhibitory systems (Hagiwara et al., 2009).

Cumulating evidence shows neuroglia can closely interacted with sensitized neurons under neuropathic pain conditions (Watkins et al., 2001; Scholz and Woolf, 2007; Milligan and Watkins, 2009). Activation of mitogen-activated protein kinases (MAPKs) in spinal neurons and glia can regulate nociceptive processes, that is initiation, development and maintenance, and become the hallmarks of central sensitization. Phosphorylated-MAPKs (p-ERK, p-p38 and p-JNK) can induce downstream intracellular molecules (Zhuang et al., 2006; Suter et al., 2007; Wen et al., 2011) and excite exocrine releases of proinflammatory cytokines including IL-1β, IL-6 and TNF-α to enhance hyperalgesia in neuropathic or inflammatory pain (Tsuda et al., 2004; Scholz and Woolf, 2007; Suter et al., 2007; Ji et al., 2009). Accordingly, levels of p-ERK and p-p38 can serve as molecular markers to indicate cellular responsiveness to pain and treatment.

The present study is to elucidate the effect of PRF on nerve injury-induced pain behaviours at the early post-injury stage and possible inhibition on spinal MAPKs activation. In a spinal nerve ligation (SNL) model, we investigated whether early PRF stimulation at DRG could suppress acute neuropathic pain, inhibit injury-induced MAPKs activation and modulate glia-activated inflammatory substances in the spinal cord.

2. Materials and methods

2.1 Animal preparation

Experiments were performed in adult male Sprague-Dawley rats (220–250 g; BioLASCO, Taiwan Co., Ltd.; Ilan, Taiwan). Animals were housed in groups of two to three in plastic cages with soft bedding and acclimatized to the animal facilities (22 ± 0.5°C, relative humidity 40–60%, 8:00 a.m. to 8:00 p.m. alternate light-dark cycles, food and water *ad libitum*) for at least 3 days. Experiments were performed between 9:00 a.m. to 5:00 p.m. The study protocols were approved by the Institutional Animal Care and Utilization Committee, Shin-Kong Wu Ho-Su Memorial Hospital, Taipei, Taiwan and China Medical University Hospital, Taichung, Taiwan. All experiments followed the 'Ethical guidelines for the treatment of animals of the International Association for the Study of Pain' (Zimmermann, 1983). Efforts were made to minimize animal number and suffering.

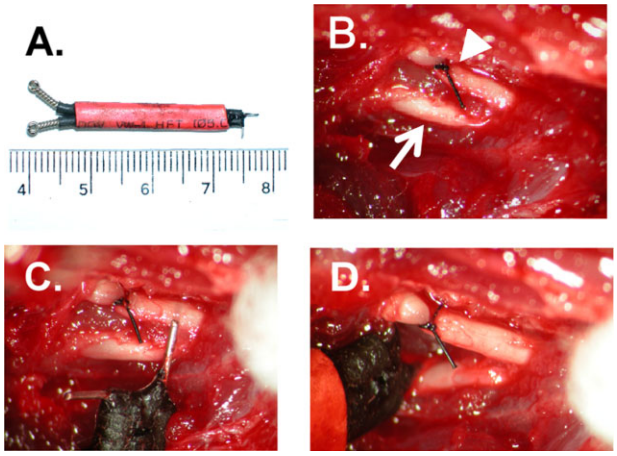

Figure 1 A specially designed pulsed radiofrequency (PRF) electrode and the spinal nerve ligation (SNL)-induced pain model. (A) The bipolar needle electrode; (B) the exposure of intact L4 (arrow) and ligated L5 spinal nerves (arrowhead) after cut of the L5 transverse process; (C) the electrode and the nerves; (D) one probe of the electrode was inserted into L5 intervertebral foramen and the other unseen probe was placed inside deeper tissues.

2.2 A novel design of a PRF system

The specially designed PRF delivery system has been previously reported (Chiu et al., 2010) and was modified in this study.

Two 32 g stainless steel needles were insulated with a heat shrinkable pyrocondensation tube and were bound together except for the distal 3-mm tips (Fig. 1A). The needle tips were blunted; one exposed tip was bended 105° upward to be inserted into the foramen, and the other straight tip was in contact with the surrounding non-neural tissues as a grounding electrode (Fig. 1C–D). The electrode was connected to a PXI-5402 Function Generator (National Instruments, Austin, TX, USA). PRF parameters were based on clinical settings. They were 25-ms biphasic pulses/trains at 2-Hz frequency and each pulse/train was composed of 500-KHz sinusoid radiofrequency (RF) waves. PRF duration was totally 300 s. The temperature of the electrode system was always below 38°C. Direct current levels of the biphasic pulses/trains were kept at zero voltage to avoid charge unbalanced. Different from clinical setting, the stimulating intensity was ± 2.5 V and was much lower than that about 40–50 V in human (Chiu et al., 2010).

2.3 Surgeries

2.3.1 SNL

Under anaesthesia of 2% isoflurane, a 3-cm skin incision was made between the left iliac crest and the lower lumbar spine. The muscles within the space and the L5 transverse process were removed to expose L4 and L5 spinal nerves and L5 intervertebral foramen (Fig. 1B). The L5 spinal nerve was identified and tightly ligated with 6-0 silk thread (Kim and Chung, 1992; Li et al., 2000). Haemostasis was performed, and the deep paraspinal muscles and superficial back muscles were sutured by layers. The skin was closed with stitches.

2.3.2 PRF electrode placement and 'test stimulation' at L5DRG

The PRF electrode was carefully inserted into the L5 foramen (Fig. 1C and D) after L5 ligation. A 'test stimulation' produced a characteristic pattern of limb twitches by contracting the anterior tibial muscles. The minimal intensity was 0.25–0.3 V at 0.5 ms, 2 Hz square-wave pulses (Grass S88 electrostimulator, Astro-med, Grass, West Warwick, RI, USA). Any different patterns of hind limb movement, such as tail flick or abduction and flexion of the fifth toe, indicated incorrect electrode placement. The electrode handle was securely hand-held and connected to the PRF power generator. After 5-min PRF stimulation, the electrode was removed. The experimenter who performed PRF stimulation was trained to safely conduct these procedures (Protasoni et al., 2009).

2.4 Nociceptive evaluation

2.4.1 Mechanical responses by von Frey test

Animals were individually placed in a Plexiglas cage chamber (10 x 12 x 20 cm) on an elevated iron mesh floor once daily from 3 to 4 days before surgery to habituate them to the testing environment. A series of von Frey filaments (Stoelting, Wood Dale, IL, USA; 0.4, 0.6, 1, 2, 4, 8, 15 and 26 g, and starting from the 4 g) were sequentially presented to perpendicularly stimulate the plantar surface at the left hind paw for 5–6 s using an up-down method (Chaplan et al., 1994). The value of threshold was an average of two measurements, separated by at least 5 min, at each time point calculated through 50% withdrawal threshold (Dixon, 1980). The animals were tested daily from 2 days before surgery as baselines, and then 1, 3, 5 and 7 days after operation.

2.4.2 Thermal responses by plantar withdrawal test

Rats were placed individually in the plantar test device (Plantar Test Apparatus, IITC, Victory Blvd Woodland Hills, CA, USA) with a glass floor pre-warmed to a constant 30°C. After 15-min acclimation, a focused radiant heat source underneath the glass floor was projected to the paws. The basal emitting heat was adjusted to produce withdrawal latencies of 15–20 s in normal rats and was removed at a cut-off latency of 25 s to avoid paw injury. Each rat was tested three times at an interval of 5 min, and the measurements were averaged to be the withdrawal latency. Data were obtained at time points the same as the above.

Mechanical and thermal tests were conducted in order on the same day with a 1-h interval between. The experimenters who performed the tests were blind to the group allocation of the rats.

2.5 Immunohistochemical analysis

Animals were deeply anaesthetized under a high concentration of isoflurane, thoracotomized and transcardially perfused with 200 mL of 37°C saline followed by 300 mL of 4°C, 4% paraformaldehyde in 0.1 M phosphate buffer (PB). The L4–5 spinal segments were carefully removed after laminectomy, post-fixed overnight and then cryoprotected in cold 30% sucrose/PB overnight. Transverse sample sections (30 μm in thickness) were cut in a cryostat. After blocking with 2% normal goat serum containing 0.3% Triton X-100 for 1 h at room temperature, sections were incubated with primary antibody at 4°C for one or two nights. Sections were then incubated with biotinylated goat anti-rabbit IgG (1:200, Vector Laboratories, Burlingame, CA, USA) for 2 h and subsequently with ExtraAvidin peroxidase (1:1000, Sigma-Aldrich, St. Louis, MO, USA) for 1 h. After repeated PB rinsing, sections were reacted with diaminobenzidine in PB containing H_2O_2 for 6 min. Spinal free-floating sections were mounted onto gelatin-coated glass slides, air-dried and coverslipped. For double immunofluorescence, sections were incubated with a mixture of two primary antibodies from different species at 4°C, followed by a mixture of FITC- and Cy3-conjugated secondary antibodies (Jackson ImmunoResearch, West Grove, PA, USA). The stained sections were examined with Zeiss Axio Imager A2 microscopy (Göttingen, Lower Saxony, Germany) and images were captured with a charge-coupled device camera (RoHS, Qimaging; Media Cybernetics, Bethesda, MD, USA).

For statistical analysis, only clearly expressed immunoreactive cells were counted. At a magnification of ×100, positive cells in the dorsal horn were calculated by laminae (I–V) on randomly chosen sections, at least eight for each spinal segment, and the numbers were averaged to represent segmental expressions.

The primary antibodies included a rabbit monoclonal anti-phospho-ERK (1:400; Cell Signaling Technology, Danvers, MA, USA), rabbit polyclonal anti-phospho-p38 MAPK (1:400; Cell Signaling Technology), goat polyclonal anti-TNF-α (1:300; R&D Systems, Minneapolis, MN, USA) mouse monoclonal neuronal specific nuclear protein (NeuN, a neuronal marker, 1:1500; Chemicon, Temecula, CA, USA), mouse polyclonal anti-glial fibrillary acidic protein (GFAP) (astrocyte marker, 1:6000; Chemicon) and mouse monoclonal anti-OX-42 (CD11b, microglia marker, 1:200; Serotec, Indianapolis, IN, USA).

2.6 Study design and group allocation

Nociceptive responses, MAPK activations,and TNF-α expression were used in this study to approach PRF's effect on neuropathic pain. Rats were randomly allocated into three groups: (1) the PRF group: Rats were subjected to a sham SNL surgery, that is removal of L5 transverse process to expose the L4 and L5 spinal nerves but no nerve ligation. PRF stimulation at L5 DRG was conducted; (2) the SNL group: SNL surgery followed by electrode placement without electrical stimulation; and (3) the SNL+PRF group: SNL followed by 300-s PRF stimulation. Rats were killed at predetermined time points for staining analyses.

2.7 Statistical analysis

Data are reported as mean ± standard error of the means. Comparisons for behavioural data or immunoreactive (ir) cell count were made by a two-way analysis of variance (ANOVA) with repeated measures to compare the groups over all times. The factors analysed were treatment, time and treatment × time interaction. In the case of the treatment × time interaction, a one-way ANOVA followed by *post hoc* Tukey's test was performed for each time point. Value differences between baseline and multiple time points were analysed by repeated-measure ANOVA followed by Tukey's test (Statistical Software Package PRISM v.2; GraphPad Software, Inc., La Jolla, CA, USA). A value of $p < 0.05$ was regarded as statistically significant.

3. Results

3.1 A pilot study

A pilot study was conducted beforehand and an optimized system was designed to be applied in rats for the following reasons. First, a miniature electrode was created to replace clinical straight RF needle because the later is too large-bore to be inserted into the tiny intervertebral foramen in rats. Second, PRF intensity at 40–45 V in human may be too strong for rats. In our pilot study, vigorous twitches in rat's hind leg were observed when DRG was stimulated by PRF generator (NT2000 RF Generator, Neurotherm®, Wilmington, MA, USA) at 45 V, whereas this response is seldom seen in human. Electrical impedance may be part of the cause. Electric impedance is in proportion to the distance between the electrode and the ground pad, and obviously the distance for a bipolar circuit is ten times greater than it is for unipolar stimulation. Third, many clinical RF machines have prefixed stimulating parameters. Changeable electric variables for experimental needs are difficult to obtain. Accordingly, we fabricated a new bipolar stimulating electrode and a different power generator.

3.2 PRF treatment suppressed SNL-induced nociceptive hypersensitivity

SNL induced significant mechanical and thermal pain. Withdrawal responses to von Frey fibres dropped

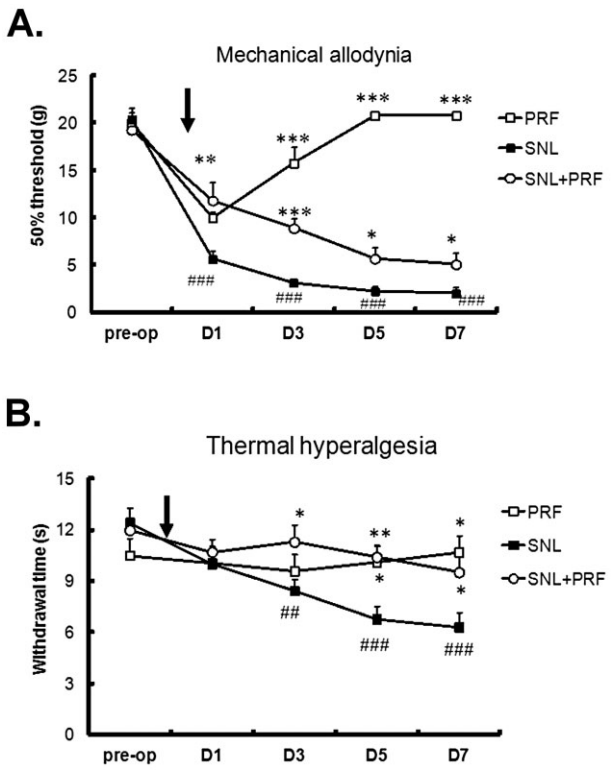

Figure 2 Behavioural responses in the rats subjected to the sham operation with pulsed radiofrequency (PRF; the PRF group), spinal nerve ligation (SNL) without PRF (the SNL group), or SNL plus PRF (the SNL + PRF group) stimulation. Tactile allodynia and thermal hyperalgesia were evaluated by von Frey test (A) and heat withdrawal test (B), respectively. D, Day; Arrows, indicating PRF stimulation. One-way analysis of variance (ANOVA) with *post hoc* Tukey's test, * $p < 0.05$, ** $p < 0.01$, *** $p < 0.001$ for PRF or SNL + PRF versus SNL. Repeated-measure ANOVA for time course change in the SNL group, ## $p < 0.01$, ### $p < 0.001$ for data versus pre-op baseline. $n = 6, 9, 10$ for PRF, SNL and SNL + PRF, respectively.

from pre-ligation baseline (pre-op) 20.45 ± 1.10 g to 5.68 ± 0.76 g on day 1 and to a constant level below 3 g afterwards (all $p = 0.000$ vs. pre-op; repeated-measure ANOVA, Fig. 2A). Meanwhile, thermal hyperalgesia appeared slowly over 7 days. Heat thresholds dropped from pre-op 12.41 ± 0.88 s to 6.29 ± 0.87 s on day 7 after SNL ($p = 0.000$, repeated measure ANOVA; Fig. 2B). Treatment with 5-min PRF stimulation at the L5 DRG significantly reduced mechanical hypersensitivity for 7 days from day 1 ($p < 0.01$ for SNL+PRF vs. SNL, Fig. 2A), day 3 ($p < 0.001$), day 5 ($p < 0.05$), to day 7 ($p < 0.05$). Heat analgesia appeared later and a significant effect started on the third day (11.29 ± 1.01 s vs. 8.42 ± 0.66 s for SNL+PRF vs. SNL, $p = 0.004$) and sustained to the seventh day ($p < 0.05$; Fig. 2B). The PRF group showed no time point change different from baseline in heat thresholds and on days 3–7 in mechanical thresholds. Behaviourally, low-volt PRF attenuated SNL-induced mechanical and thermal pain.

3.3 SNL-induced ERK activation in spinal dorsal horn

Consistent with previous report (Ji et al., 1999), p-ERK appeared early at 30 min after SNL and was found in the superficial lamina (Fig. 3). By time sequence, p-ERK was shown exclusively colocalized with NeuN (neurons) at the first 30 min (Fig. 3A), and then co-expressed with NeuN or GFAP (astrocyte) in superficial and deeper laminae on day 3 (Fig. 3B). This finding of cell-type shift had been reported (Zhuang

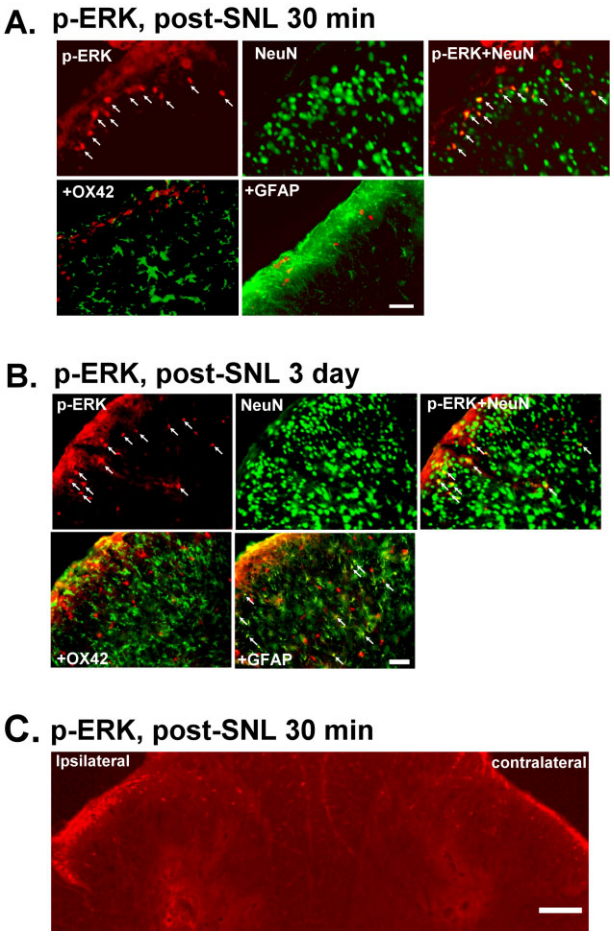

Figure 3 SNL induced ERK MAPK activation in the spinal dorsal horn. Immunofluorescence showed red for p-ERK, green for NeuN, OX-42, or GFAP staining, and orange-yellow for colocalization. (A) Double labelling at 30 min after SNL. p-ERK are exclusively colocalized with NeuN (neuron), but not with OX42 (microglia) or GFAP (astrocytes). (B) Double labelling 3 days after SNL. p-ERK are colocalized with either NeuN or GFAP, but not with OX42. White arrows, colocalization; scale bar: 50 μm. (C) p-ERK staining in bilateral dorsal horns 30 min after SNL. Scale bar: 100 μm.

et al., 2005). Although p-ERK expression was majorly shown at the lesion-ipsilateral side, there were very few p-ERK-ir cells (less than five) at the contralateral side (Fig. 3C).

3.4 SNL-induced p38 activation in spinal dorsal horn

p-p38 was found to consistently co-express with OX-42 (microglia), but not with NeuN or GFAP on day 3 (Fig. 4A) or any other time points (images not shown). p-p38-ir cells markedly increased in the dorsal horns at the ligation-side, compared to a mild-to-moderate increase at the contralateral side (Fig. 4B). Because p38 activation is often associated with microgliosis, we found high OX42 expression bilaterally 3 days after SNL, but still a stronger expression was present at the ipsilateral side compared to the other side (Fig. 4C).

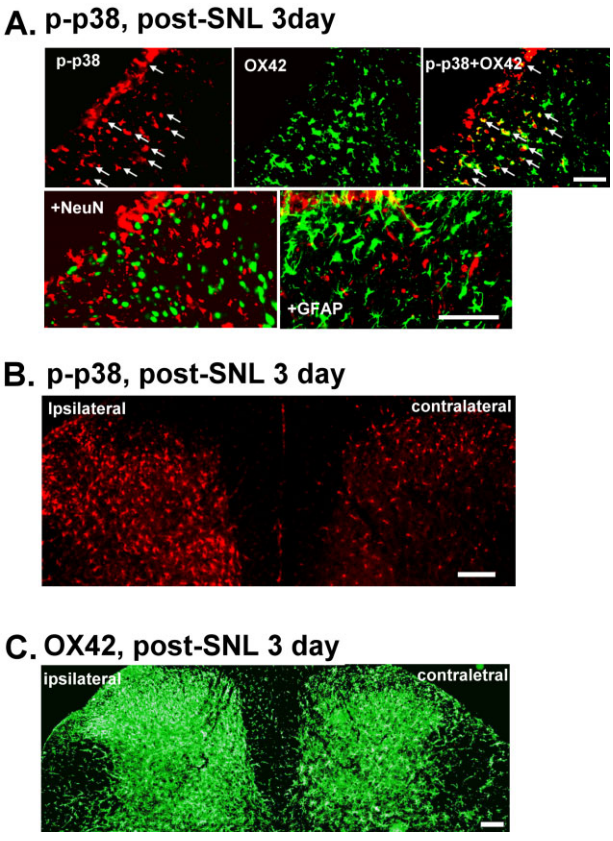

Figure 4 SNL induced p38 MAPK activation in the spinal dorsal horn. (A) Double labelling on day 3 after SNL showed p-p38 (red) was colocalized with OX42, but not with NeuN or GFAP. White arrows, colocalization; scale bar: 50 μm. (B) p-p38 staining at bilateral dorsal horns 3 days after SNL. Scale bar: 100 μm. (C) OX42 staining at bilateral dorsal horns 3 days after SNL. Scale bar: 100 μm.

3.5 PRF inhibited SNL-induced spinal p-ERK at early 30 min and the third day

We examined the level above the injury, L4, and the injury level, L5 for changes in expression of p-ERK. Peripheral nerve injury usually induces characteristic expansion of receptive field in the spinal segments above and below the injured dermatonal segment. The mechanism why L4 segment is involved was explained by previous studies (Li et al., 2000; Ji and Woolf, 2001; Wen et al., 2007).

In the SNL group, p-ERK-ir cells appeared as early as post-operation 30 min in outer one-third of the superficial lamina (Fig. 5A), and persisted high till day 7 (about 30–40/segment at any time points, Fig. 5B–D). Very few p-ERK-ir cells were present in ipsilateral deeper laminae (III–V). PRF stimulation (SNL+PRF) significantly reduced p-ERK numbers in the superficial lamina of L4 at 30 min and of L4–L5 on day 3 (Fig. 5B–C). No PRF effect was found 7 days after SNL (Fig. 5D). Notably, the sham surgery with PRF (PRF) led to relatively lesser ERK activation compared to those in other groups. (Fig. 5B–D). The numbers of p-ERK-ir cells did not differ between the L4 and L5 segments for any group or at any time point.

3.6 PRF decreased SNL-increased p-p38 immunoreactive cells in spinal microglia

We found evident increases of p-p38 in both the SNL and SNL+PRF group, compared to very few p-p38 in the PRF group (Fig. 6A). p-p38 appeared as early as post-SNL 30 min, reached peak on day 3, and gradually declined on day 7 (Fig. 6B–D).

PRF treatment significantly reduced p-p38 at the 30 min, on the third and the seventh day. The differences were shown in deep lamina of L4 at 30 min, in superficial lamina of L4 and L5 on day 3, and in superficial lamina of L5 on day 7 (all $p < 0.05$ for SNL+PRF vs. SNL, Fig. 6B–D). The PRF effect is most evident on the third day because p-p38 in both L4 and L5 was significantly inhibited. The PRF group showed relatively few p-p38 at all days except day 7 (Fig. 6B–D). Notably, there was no segmental difference in the expressive pattern and number of p-p38-ir cells between L4 and L5 segments at any time point (Fig. 6A–D).

3.7 PRF suppressed TNF-α expression after nerve injury

Spinal TNF-α serves as either an upstream activator or a downstream product in p-p38-mediated neuroin-

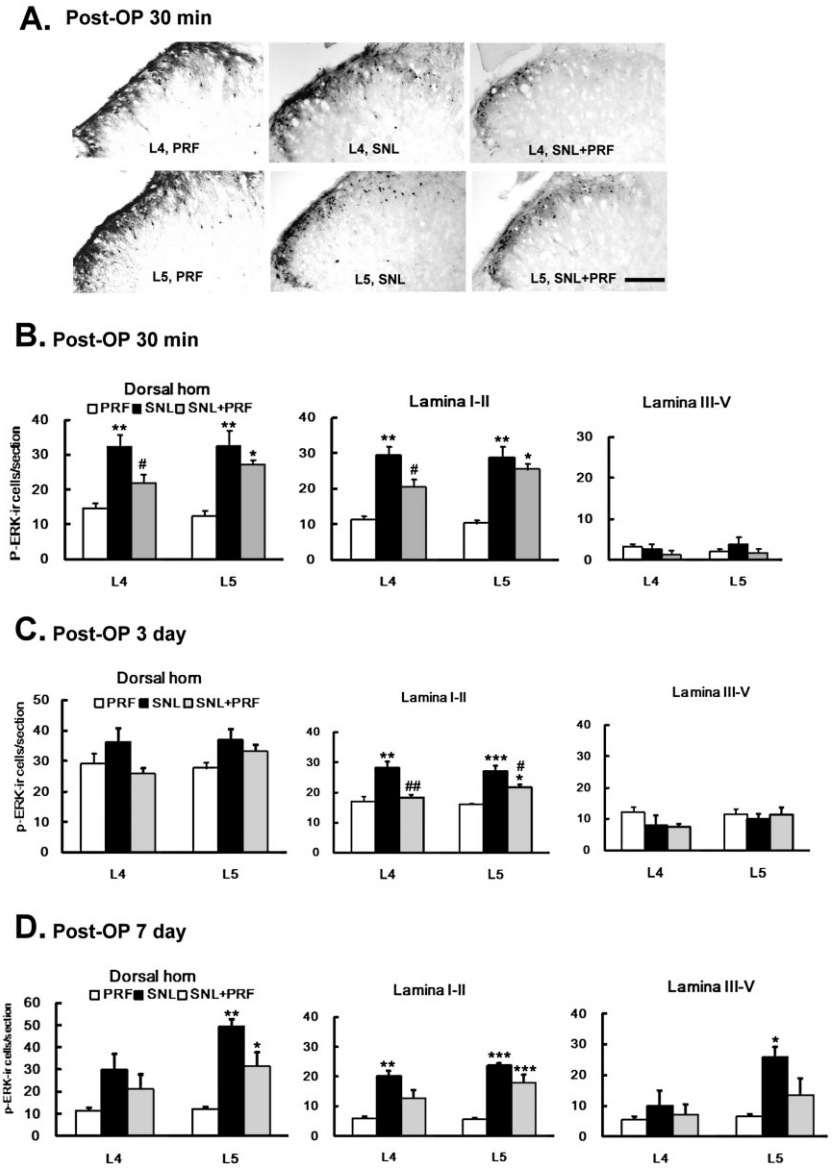

Figure 5 Effect of PRF on p-ERK induction after SNL. (A) p-ERK-ir distribution in the PRF (sham SNL with PRF), SNL, and SNL+PRF group at 30 min after operation (post-OP). Upper panels, L4 spinal dorsal horn; lower panels, L5 spinal dorsal horn. Scale bar: 100 μm. (B)–(D) Comparison of p-ERK-ir cell numbers among the PRF, SNL and SNL + PRF groups. Data were analysed by laminae, by spinal segment and by different time points. Laminae I–II: superficial lamina. One-way analysis of variance with *post hoc* Tukey's test, * $p < 0.05$, ** $p < 0.01$, *** $p < 0.001$ versus PRF; # $p < 0.05$, ## $p < 0.01$ for SNL + PRF versus SNL. Rat number = 3–5 for the PRF, 6–8 for the SNL, 5–7 for the SNL + PRF at individual time point.

flammatory signal cascade within activated microglia after nerve injury (Schafers et al., 2003; Wen et al., 2011). Hence, TNF-α expression was examined on the first and seventh post-SNL day. We found that TNF-α-ir cells were densely distributed in laminae I–III in the L4 and L5 dorsal horns (Fig. 7-A.a). Therefore, we counted all immunoreactive cells within this area for group comparison. Relatively fewer positive cells were found in the PRF group (Fig. 7-A.b). On the first post-operative days, the number of TNF-α-ir cells in the SNL group (213.67 ± 25.54) was significantly higher than those in the PRF group (100.92 ± 13.42, $p < 0.05$) and those in the SNL+PRF group (131.92 ± 4.29, $p < 0.05$). On the seventh day, TNF-α expression decreased in all groups. However, the SNL group still showed significantly higher TNF-α-positive number than the PRF group ($p < 0.01$) and the SNL+PRF group ($p < 0.05$) (Fig. 7B). It was clear that PRF treatment suppressed the TNF-α levels on the first and seventh post-operative days.

4. Discussion

To our knowledge, this study is the first to report the relationship between MAPKs activation and PRF stimulation. Our findings demonstrated that early application of PRF adjacent to the DRG significantly diminished nerve ligation-induced mechanical allody-

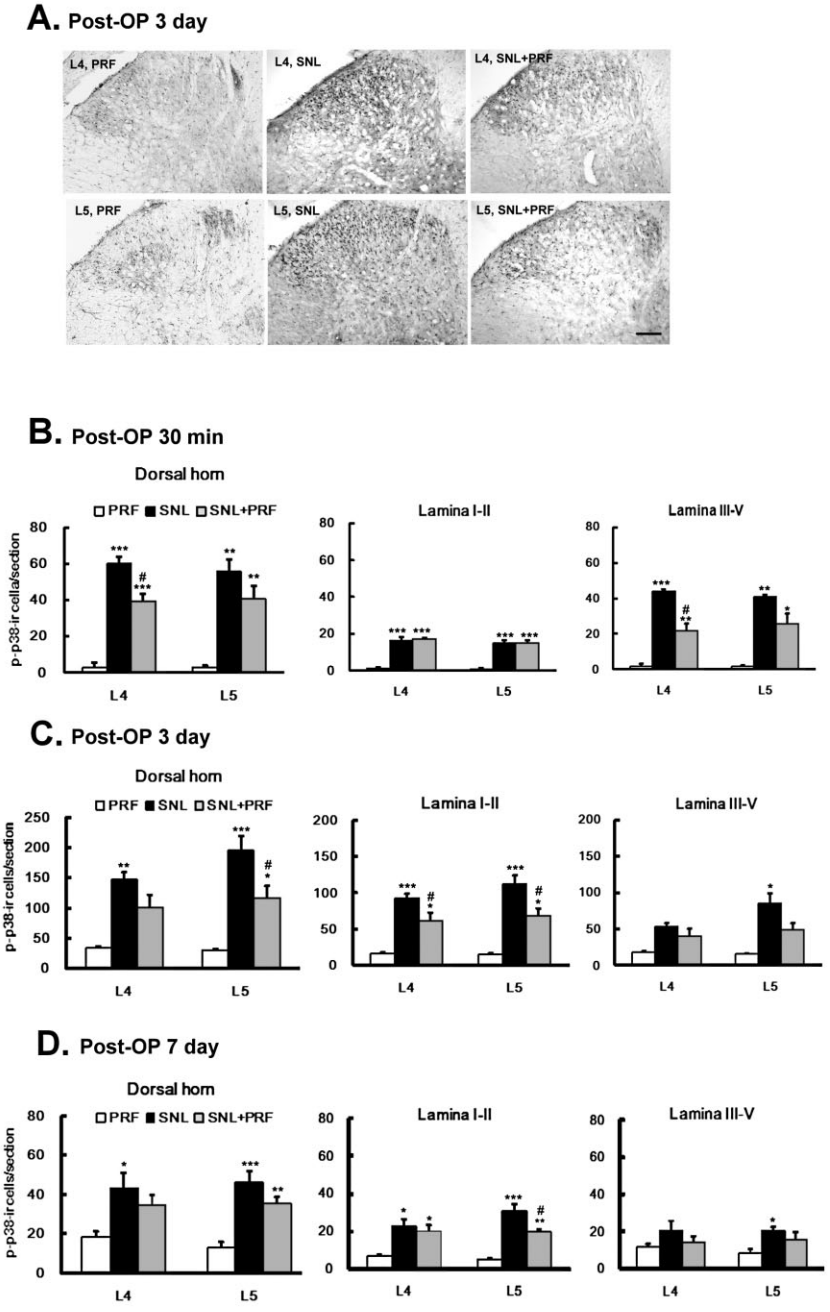

Figure 6 Effect of PRF on p38 activation after SNL. (A) p-p38-ir distribution in the PRF (sham SNL with PRF), SNL and SNL + PRF group at 3 day after operation (post-OP). Upper panels, L4 spinal dorsal horn; lower panels, L5 spinal dorsal horn. Scale bar: 100 μm. (B–D) Comparison of p-p38-ir cell numbers among the PRF, SNL, and SNL + PRF groups. Data were analysed by laminae, by spinal segment and by different time points. Laminae I–II: superficial lamina. One-way analysis of variance with *post hoc* Tukey's test, * $p < 0.05$, ** $p < 0.01$, *** $p < 0.001$ versus PRF; # $p < 0.05$ for SNL + PRF versus SNL. Rat number = 3–5 for the PRF, 6–8 for the SNL, 5–7 for the SNL + PRF at individual time point.

nia for 7 days and thermal hyperalgesia on post-operative day 3–7. In the spinal levels, PRF suppressed p-ERK in the sensitized neurons and glia, p-p38 in the activated microglia, and TNF-α expression in the dorsal horns. Our findings indicated that single stimulation with low-voltage PRF can effectively ameliorate early nociceptive behaviours and spinal MAPK activations.

A distinct finding in this study is an acute effect of PRF can occur in early neuropathic pain. In human, PRF was usually applied to treat chronic neuropathic pain and reported to have analgesic effect ranged from weeks to over 6 months with over 50% pain relief (Cahana et al., 2006; Malik and Benzon, 2008). Mechanisms regarding PRF treatment at the early stage of nerve injury are much less understood. Therefore, a comparison between the present study and other animal studies with PRF application in neuropathic pain states has to be careful because underlying mechanisms of neuropathic pain at early versus late stages may differ.

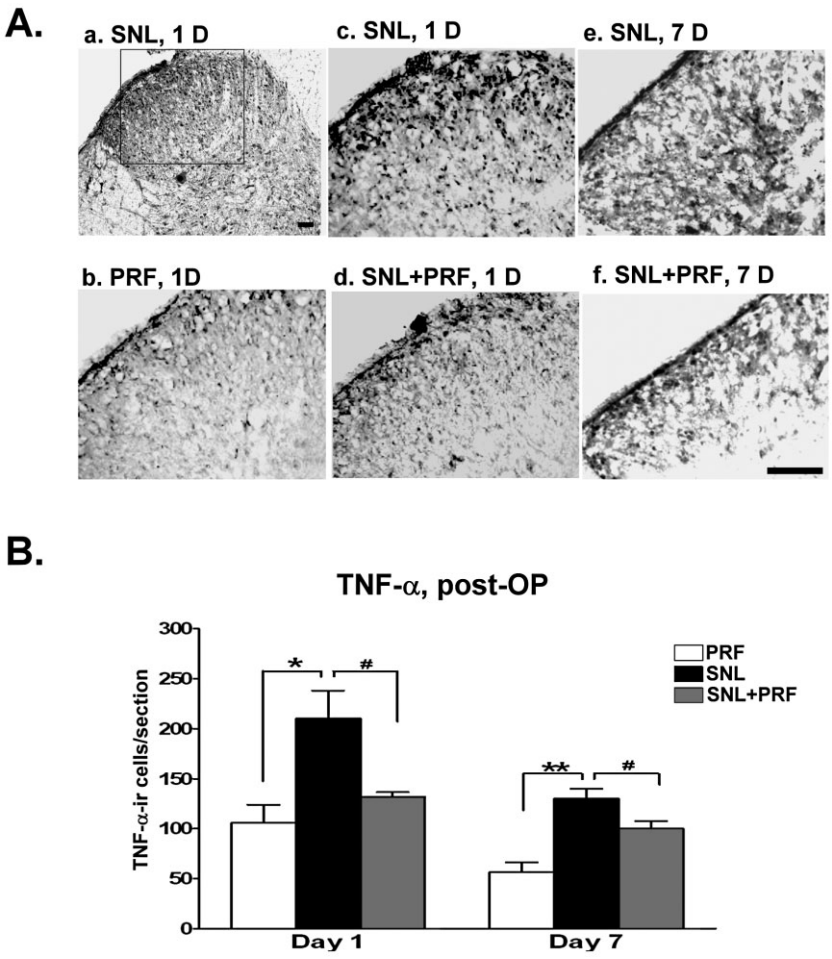

Figure 7 Effect of PRF on spinal TNF-α expression after SNL. (A) TNF-α expression in the spinal dorsal horns in different groups and time points. (a): An example of a preset square is shown on a lower magnified image. Only TNF-α-ir cells within this square were counted for analysis. (b–d): TNF-α on day 1; (e, f): TNF-α on day 7. Scale bars: 100 μm. (B) Calculation of TNF-α-ir cells on post-op day 1 and 7. Rat number = 5/group. One-way analysis of variance with Tukey's test, * $p < 0.05$, ** $p < 0.01$ versus PRF; # $p < 0.05$ for SNL + PRF versus SNL.

We observed that the analgesic effect in this study is shorter than those in previous animal studies. Differences in pain stage or in PRF protocols may affect outcomes. In a rabbit model of partial sciatic nerve injury, repeated PRF stimulations at DRGs reduced punctuate hyperalgesia for 3 weeks and heat hyperalgesia for 2 weeks (Aksu et al., 2010). PRF stimulating at DRG in a SNL model showed a slow onset, discontinued anti-allodynic effect on 10 days of the first 14 post-PRF days and another moderate-to-strong effect after day 32 (Perret et al., 2011). In both above studies, PRF was applied at least 10 days after nerve injury when neuropathic pain had been well developed. Another difference has to be noted. After nerve injury, early PRF application produced analgesia within 1 day in this study, whereas late PRF application had a few days delay of analgesic effect (Aksu et al., 2010; Perret et al., 2011). To be precise, nerve ligation model has two modalities of pain in the beginning, that is, an inflammatory pain originated from tissue trauma and another neuropathic pain directly from nerve injury. Early PRF may induce an inhibitory effect on both conditions. A previous study of inflammatory pain showed that PRF treatment of sciatic nerve attenuated adjuvant-induced thermal hyperalgesia from day 1 to day 3 (Hagiwara et al., 2009). Collectively, it is implicated that PRF could not only attenuate pain at early or late post-injury stages, but also for different pain types.

This study revealed an inhibitory action of PRF on activations of spinal ERK and p38, two important intracellular signals to control cellular responsiveness, and strongly implicated that PRF analgesia may include down-regulation of MAPK-dependent nociceptive cascades within postsynaptic neurons and glia. Several lines of evidence indicated that p-ERK induction is closely parallel with pain initiation as evident by expression within neurons after injury, C fibre-specific stimulation and expression exclusively in laminae I and II (Ji et al., 1999; Zhuang et al., 2005; Gao and Ji, 2009). PRF may reduce neuronal p-ERK in the superficial lamina as early as 30 min, suggesting a

direct blockade of neural transmission pathway. PRF has a selective C-fibre blockade effect (Hamann et al., 2006; Aksu et al., 2010), and was further evidenced by our electrophysiological study (unpublished data) that C fibre-mediated, but not A fibre-mediated, evoked potentials were selectively suppressed as early as 30 min after PRF. In addition, ERK could be sequentially activated in neurons within 10 min after nerve injury and then in both neurons and microglia between 1 and 3 post-injury days (Zhuang et al., 2005). Our data showed that PRF suppressed p-ERK-ir cells on the third day, when p-ERK was found to co-express within neurons and astrocytes. Obviously, PRF may modulate p-ERK-dependent nociceptive sensitizations in spinal neurons and astrocytes.

Furthermore, p38 MAPK plays an equally important role. Activation of p38 was shown to contribute to neuropathic pain development (Suter et al., 2007; Wen et al., 2007). SNL activated microglial p-p38, which reached peak on the third day, and kept at high levels for weeks (Jin et al., 2003). PRF maximally suppressed microglial p-p38 during the third to seventh day, in agreement with the time course of p38-dependent signal sensitization. In fact, the prolonged analgesia of single PRF stimulation outlasts the duration of single injection of p38 inhibitors (Wen et al., 2007, 2009). Besides, persistent inputs from injury could reorganize nociceptive receptive field in the spinal cord (Suzuki et al., 2000; Ririe et al., 2008), and p38 activation is involved in expansion of receptive field during central sensitization (Xie et al., 2007). Suppression of p-p38 in L4 and L5 by PRF may lower spill-over of microglia-released inflammatory substances, and subsequently reduce recruitment of previously inactive cells in adjacent spinal segments. Significant inhibition of p-ERK in laminae I–II on the third day may synergistically modulate this neuroplasticity.

The lower TNF-α production in the SNL+PRF group on day 1 and day 7 supports PRF may contribute to modulate pain circuitry within neuron and glia. TNF-α is produced by various cells, including immune cells, neurons and neuroglia, and was proved to alter nociceptive hypersensitivity in different pain models (Svensson et al., 2005; Loram et al., 2007; Wen et al., 2011). TNF-α levels increases drastically within hours at the injured nerves and related DRGs (Lee et al., 2004; Sacerdote et al., 2008; Rothman et al., 2009), and released TNF-α can be served as an upstream activator of spinal p38 MAPK to enhance pathological pain states (Schafers et al., 2003; Svensson et al., 2005; Boyle et al., 2006). Intrathecal injection of TNF-α neutralizing blocker prevented spinal p-p38 and allodynia after SNL or spinal cord injury (Schafers et al., 2003; Svensson et al., 2005; Marchand et al., 2009). On the other hand, activation of P2X7 receptors on microglia increased ERK- and p38-dependent TNF production (Suzuki et al., 2004; Lister et al., 2007), and p38 inhibitor prevented nucleocytoplamic transport of TNF mRNA (Suzuki et al., 2004). Sensitivity of TNF-α receptor-expressed neurons is also enhanced. In a patch-clamp study, frequencies of excitatory postsynaptic current were robustly increased in TNF-α-perfused spinal neurons of wild-type slices, but were almost abolished in TNF-αR1 knock-out neurons (Zhang et al., 2011). Together with our findings that PRF inhibited TNF-α expression on the first and seventh days, it is convincing that PRF can depress neuron/glia/cytokines-mediated nociceptive signals to diminish neuropathic pain development.

The bipolar RF design in this study may yield important influence on analgesic quality. The electric physics generated by RF with a bipolar stimulation and low-voltage (5 V) intensity could be different in nature from that of a clinical unipolar, high-voltage (35–45 V) stimulation. Many studies indicated that neuromodulation induced by PRF-generated electric field (E-field) is more prominent than that by PRF-produced thermal action (Cosman and Cosman, 2005; Chua et al., 2011). Pulsed E-field could modulate gene expression and molecular signals in stimulated DRG (Sandkuhler et al., 1997) thru rectifying cell membrane potential for synaptic depolarization (Cosman and Cosman, 2005). Meanwhile, the temperature of the electrode tip measured in this system is low (< 39°C) (Chiu et al., 2010), so short heat spikes at the needle tip are unlikely to cause thermal injury (Erdine et al., 2009). However, when a bipolar PRF electrode imposes on the DRG, the E-field is densely distributed within a very narrow range. Therefore, the reduced neuron/glia/MAPK activations in the spinal cord should be more complex in mechanisms than a direct effect of E-field on the cord. Similarly, comparing efficacy between bipolar and unipolar PRF required more evidence because variables such as electrode size, PRF parameters and stimulation position may be all involved to influence the results.

5. Conclusions

Taken together, we demonstrated in this study that single application of low-voltage PRF treatment ameliorated acute neuropathic pain state for 7 days and modulated MAPK-dependent spinal sensitization. This

preclinical study suggests that early PRF treatment may be feasible to reduce pain complication in acute peripheral nerve injury.

Acknowledgements

We have special thanks to Prof. Ching-Yuang Lin (Clinical Immunology Center, China Medical University Hospital, Taiwan; College of Medicine, China Medical University, Taiwan) for his critical reviewing of this manuscript.

Author contributions

Y.-R.W. and C.-W.L. conceived, designed and supervised all experiments, interpreted of findings and wrote the manuscript. M.-L.L., W.-T.L. and R.-Y.H. performed experiments, acquisition of data, statistical analysis and prepared the manuscript. S.-Y.T. and G.-C.Y. helped in preparing the manuscript. T.-C.C., S.-H.H. and C.-H.C. contributed to the behavioural tests in the study. H.-W.C. contributed to the PRF stimulating device of the study. All authors read the manuscript and approved the submission.

References

Aksu, R., Ugur, F., Bicer, C., Menku, A., Guler, G., Madenoglu, H., Canpolat, D.G., Boyaci, A. (2010). The efficiency of pulsed radiofrequency application on L5 and L6 dorsal roots in rabbits developing neuropathic pain. *Reg Anesth Pain Med* 35, 11–15.

Boyle, D.L., Jones, T.L., Hammaker, D., Svensson, C.I., Rosengren, S., Albani, S., Sorkin, L., Firestein, G.S. (2006). Regulation of peripheral inflammation by spinal p38 MAP kinase in rats. *PLoS Med* 3, e338.

Cahana, A., Van Zundert, J., Macrea, L., van Kleef, M., Sluijter, M. (2006). Pulsed radiofrequency: Current clinical and biological literature available. *Pain Med* 7, 411–423.

Chaplan, S.R., Bach, F.W., Pogrel, J.W., Chung, J.M., Yaksh, T.L. (1994). Quantitative assessment of tactile allodynia in the rat paw. *J Neurosci Methods* 53, 55–63.

Chiu, H.W., Lin, M.L., Lin, C.W., Lin, W.T., Ho, I.H., Fang, P.H., Wen, Y.R., Lu, S.S. (2010). Pain control on demand based on pulsed radiofrequency stimulation of the dorsal root ganglion using a batteryless implantable CMOS SoC. *IEEE Trans Biomed Circuits Syst* 4, 350–359.

Chua, N.H., Vissers, K.C., Sluijter, M.E. (2011). Pulsed radiofrequency treatment in interventional pain management: Mechanisms and potential indications-a review. *Acta Neurochir (Wien)* 153, 763–771.

Cosman, E.R., Jr, Cosman, E.R., Sr. (2005). Electric and thermal field effects in tissue around radiofrequency electrodes. *Pain Med* 6, 405–424.

Dixon, W.J. (1980). Efficient analysis of experimental observations. *Annu Rev Pharmacol Toxicol* 20, 441–462.

Erdine, S., Bilir, A., Cosman, E.R., Cosman, E.R., Jr. (2009). Ultrastructural changes in axons following exposure to pulsed radiofrequency fields. *Pain Pract* 9, 407–417.

Erdine, S., Yucel, A., Cimen, A., Aydin, S., Sav, A., Bilir, A. (2005). Effects of pulsed versus conventional radiofrequency current on rabbit dorsal root ganglion morphology. *Eur J Pain* 9, 251–256.

Gao, Y.J., Ji, R.R. (2009). c-Fos and pERK, which is a better marker for neuronal activation and central sensitization after noxious stimulation and tissue injury. *Open Pain J* 2, 11–17.

Gray, P. (2008). Acute neuropathic pain: Diagnosis and treatment. *Curr Opin Anaesthesiol* 21, 590–595.

Hagiwara, S., Iwasaka, H., Takeshima, N., Noguchi, T. (2009). Mechanisms of analgesic action of pulsed radiofrequency on adjuvant-induced pain in the rat: Roles of descending adrenergic and serotonergic systems. *Eur J Pain* 13, 249–252.

Hamann, W., Abou-Sherif, S., Thompson, S., Hall, S. (2006). Pulsed radiofrequency applied to dorsal root ganglia causes a selective increase in ATF3 in small neurons. *Eur J Pain* 10, 171–176.

Higuchi, Y., Nashold, B.S., Jr, Sluijter, M., Cosman, E., Pearlstein, R.D. (2002). Exposure of the dorsal root ganglion in rats to pulsed radiofrequency currents activates dorsal horn lamina I and II neurons. *Neurosurgery* 50, 850–855.

Ji, R.R., Baba, H., Brenner, G.J., Woolf, C.J. (1999). Nociceptive-specific activation of ERK in spinal neurons contributes to pain hypersensitivity. *Nat Neurosci* 2, 1114–1119.

Ji, R.R., Gereau, R.W., Malcangio, M., Strichartz, G.R. (2009). MAP kinase and pain. *Brain Res Rev* 60, 135–148.

Ji, R.R., Woolf, C.J. (2001). Neuronal plasticity and signal transduction in nociceptive neurons: Implications for the initiation and maintenance of pathological pain. *Neurobiol Dis* 8, 1–10.

Jin, S.X., Zhuang, Z.Y., Woolf, C.J., Ji, R.R. (2003). p38 mitogen-activated protein kinase is activated after a spinal nerve ligation in spinal cord microglia and dorsal root ganglion neurons and contributes to the generation of neuropathic pain. *J Neurosci* 23, 4017–4022.

Kim, S.H., Chung, J.M. (1992). An experimental model for peripheral neuropathy produced by segmental spinal nerve ligation in the rat. *Pain* 50, 355–363.

Lee, H.L., Lee, K.M., Son, S.J., Hwang, S.H., Cho, H.J. (2004). Temporal expression of cytokines and their receptors mRNAs in a neuropathic pain model. *Neuroreport* 15, 2807–2811.

Li, Y., Dorsi, M.J., Meyer, R.A., Belzberg, A.J. (2000). Mechanical hyperalgesia after an L5 spinal nerve lesion in the rat is not dependent on input from injured nerve fibers. *Pain* 85, 493–502.

Lister, M.F., Sharkey, J., Sawatzky, D.A., Hodgkiss, J.P., Davidson, D.J., Rossi, A.G., Finlayson, K. (2007). The role of the purinergic P2X7 receptor in inflammation. *J Inflamm (Lond)* 4, 5.

Loram, L.C., Themistocleous, A.C., Fick, L.G., Kamerman, P.R. (2007). The time course of inflammatory cytokine secretion in a rat model of postoperative pain does not coincide with the onset of mechanical hyperalgesia. *Can J Physiol Pharmacol* 85, 613–620.

Malik, K., Benzon, H.T. (2008). Radiofrequency applications to dorsal root ganglia: A literature review. *Anesthesiology* 109, 527–542.

Marchand, F., Tsantoulas, C., Singh, D., Grist, J., Clark, A.K., Bradbury, E.J., McMahon, S.B. (2009). Effects of Etanercept and Minocycline in a rat model of spinal cord injury. *Eur J Pain* 13, 673–681.

Milligan, E.D., Watkins, L.R. (2009). Pathological and protective roles of glia in chronic pain. *Nat Rev Neurosci* 10, 23–36.

Perret, D.M., Kim, D.S., Li, K.W., Sinavsky, K., Newcomb, R.L., Miller, J.M., Luo, Z.D. (2011). Application of pulsed radiofrequency currents to rat dorsal root ganglia modulates nerve injury-induced tactile allodynia. *Anesth Analg* 113, 610–616.

Podhajsky, R.J., Sekiguchi, Y., Kikuchi, S., Myers, R.R. (2005). The histologic effects of pulsed and continuous radiofrequency lesions at 42 degrees C to rat dorsal root ganglion and sciatic nerve. *Spine (Phila Pa 1976)* 30, 1008–1013.

Protasoni, M., Reguzzoni, M., Sangiorgi, S., Reverberi, C., Borsani, E., Rodella, L.F., Dario, A., Tomei, G., Dell'Orbo, C. (2009). Pulsed radiofrequency effects on the lumbar ganglion of the rat dorsal root: A morphological light and transmission electron microscopy study at acute stage. *Eur Spine J* 18, 473–478.

Ririe, D.G., Bremner, L.R., Fitzgerald, M. (2008). Comparison of the immediate effects of surgical incision on dorsal horn neuronal receptive field size and responses during postnatal development. *Anesthesiology* 109, 698–706.

Rothman, S.M., Huang, Z., Lee, K.E., Weisshaar, C.L., Winkelstein, B.A. (2009). Cytokine mRNA expression in painful radiculopathy. *J Pain* 10, 90–99.

Sacerdote, P., Franchi, S., Trovato, A.E., Valsecchi, A.E., Panerai, A.E., Colleoni, M. (2008). Transient early expression of TNF-alpha in sciatic nerve and dorsal root ganglia in a mouse model of painful peripheral neuropathy. *Neurosci Lett* 436, 210–213.

Sandkuhler, J., Chen, J.G., Cheng, G., Randic, M. (1997). Low-frequency stimulation of afferent Adelta-fibers induces long-term depression at

primary afferent synapses with substantia gelatinosa neurons in the rat. *J Neurosci* 17, 6483–6491.

Schafers, M., Svensson, C.I., Sommer, C., Sorkin, L.S. (2003). Tumor necrosis factor-alpha induces mechanical allodynia after spinal nerve ligation by activation of p38 MAPK in primary sensory neurons. *J Neurosci* 23, 2517–2521.

Scholz, J., Woolf, C.J. (2007). The neuropathic pain triad: Neurons, immune cells and glia. *Nat Neurosci* 10, 1361–1368.

Sluijter, M.E. (2000). The role of radiofrequency in failed back surgery patients. *Curr Rev Pain* 4, 49–53.

Sluijter, M.E., Cosman, E.R., Rittman, I.W.B., van Kleef, M. (1998). The effects of pulsed radiofrequency field applied to the dorsal root ganglion: A preliminary report. *Pain Clinic* 11, 109–117.

Suter, M.R., Wen, Y.R., Decosterd, I., Ji, R.R. (2007). Do glial cells control pain. *Neuron Glia Biol* 3, 255–268.

Suzuki, R., Kontinen, V.K., Matthews, E., Williams, E., Dickenson, A.H. (2000). Enlargement of the receptive field size to low intensity mechanical stimulation in the rat spinal nerve ligation model of neuropathy. *Exp Neurol* 163, 408–413.

Suzuki, T., Hide, I., Ido, K., Kohsaka, S., Inoue, K., Nakata, Y. (2004). Production and release of neuroprotective tumor necrosis factor by P2X7 receptor-activated microglia. *J Neurosci* 24, 1–7.

Svensson, C.I., Schafers, M., Jones, T.L., Powell, H., Sorkin, L.S. (2005). Spinal blockade of TNF blocks spinal nerve ligation-induced increases in spinal P-p38. *Neurosci Lett* 379, 209–213.

Treede, R.D., Jensen, T.S., Campbell, J.N., Cruccu, G., Dostrovsky, J.O., Griffin, J.W., Hansson, P., Hughes, R., Nurmikko, T., Serra, J. (2008). Neuropathic pain: Redefinition and a grading system for clinical and research purposes. *Neurology* 70, 1630–1635.

Tsuda, M., Mizokoshi, A., Shigemoto-Mogami, Y., Koizumi, S., Inoue, K. (2004). Activation of p38 mitogen-activated protein kinase in spinal hyperactive microglia contributes to pain hypersensitivity following peripheral nerve injury. *Glia* 45, 89–95.

Tun, K., Cemil, B., Gurcay, A.G., Kaptanoglu, E., Sargon, M.F., Tekdemir, I., Comert, A., Kanpolat, Y. (2009). Ultrastructural evaluation of pulsed radiofrequency and conventional radiofrequency lesions in rat sciatic nerve. *Surg Neurol* 72, 496–500.

Tun, K., Savas, A., Sargon, M.F., Solaroglu, I., Kanpolat, Y. (2006). The histopathological and electron-microscopic examination of the stereotactic pulsed radiofrequency and conventional radiofrequency thermocoagulation lesions in rat brain. *Neurol Res* 28, 841–844.

Van Boxem, K., Cheng, J., Patijn, J., van Kleef, M., Lataster, A., Mekhail, N., Van Zundert, J. (2010). 11. Lumbosacral radicular pain. *Pain Pract* 10, 339–358.

van Boxem, K., van Eerd, M., Brinkhuizen, T., Patijn, J., van Kleef, M., van Zundert, J. (2008). Radiofrequency and pulsed radiofrequency treatment of chronic pain syndromes: The available evidence. *Pain Pract* 8, 385–393.

Van Zundert, J., de Louw, A.J., Joosten, E.A., Kessels, A.G., Honig, W., Dederen, P.J., Veening, J.G., Vles, J.S., van Kleef, M. (2005). Pulsed and continuous radiofrequency current adjacent to the cervical dorsal root ganglion of the rat induces late cellular activity in the dorsal horn. *Anesthesiology* 102, 125–131.

Van Zundert, J., Huntoon, M., Patijn, J., Lataster, A., Mekhail, N., van Kleef, M. (2010). 4. Cervical radicular pain. *Pain Pract* 10, 1–17.

Watkins, L.R., Milligan, E.D., Maier, S.F. (2001). Glial activation: A driving force for pathological pain. *Trends Neurosci* 24, 450–455.

Wen, Y.R., Suter, M.R., Ji, R.R., Yeh, G.C., Wu, Y.S., Wang, K.C., Kohno, T., Sun, W.Z., Wang, C.C. (2009). Activation of p38 mitogen-activated protein kinase in spinal microglia contributes to incision-induced mechanical allodynia. *Anesthesiology* 110, 155–165.

Wen, Y.R., Suter, M.R., Kawasaki, Y., Huang, J., Pertin, M., Kohno, T., Berde, C.B., Decosterd, I., Ji, R.-R. (2007). Nerve conduction blockade in the sciatic nerve prevents but does not reverse the activation of p38 mitogen-activated protein kinase in spinal microglia in the rat spared nerve injury model. *Anesthesiology* 107, 312–321.

Wen, Y.R., Tan, P.H., Cheng, J.K., Liu, Y.C., Ji, R.R. (2011). Microglia: A promising target for treating neuropathic and postoperative pain, and morphine tolerance. *J Formos Med Assoc* 110, 487–494.

Xie, Y.F., Zhang, S., Chiang, C.Y., Hu, J.W., Dostrovsky, J.O., Sessle, B.J. (2007). Involvement of glia in central sensitization in trigeminal subnucleus caudalis (medullary dorsal horn). *Brain Behav Immun* 21, 634–641.

Zhang, L., Berta, T., Xu, Z.Z., Liu, T., Park, J.Y., Ji, R.R. (2011). TNF-alpha contributes to spinal cord synaptic plasticity and inflammatory pain: Distinct role of TNF receptor subtypes 1 and 2. *Pain* 152, 419–427.

Zhuang, Z.Y., Gerner, P., Woolf, C.J., Ji, R.R. (2005). ERK is sequentially activated in neurons, microglia, and astrocytes by spinal nerve ligation and contributes to mechanical allodynia in this neuropathic pain model. *Pain* 114, 149–159.

Zhuang, Z.Y., Wen, Y.R., Zhang, D.R., Borsello, T., Bonny, C., Strichartz, G.R., Decosterd, I., Ji, R.R. (2006). A peptide c-Jun N-terminal kinase (JNK) inhibitor blocks mechanical allodynia after spinal nerve ligation: Respective roles of JNK activation in primary sensory neurons and spinal astrocytes for neuropathic pain development and maintenance. *J Neurosci* 26, 3551–3560.

Zimmermann, M. (1983). Ethical guidelines for investigations of experimental pain in conscious animals. *Pain* 16, 109–110.

